arXiv:0908.0562v1 [astro-ph.SR] 4 Aug 2009

On the solar origin of the signal at 220.7μHz: A possible component of a g mode?

A. Jiménez[1], R. A. García[2]

ABSTRACT

Gravity modes in the Sun have been the object of a long and difficult search in recent decades. Thanks to the data accumulated with the last generation of instruments (BiSON, GONG and three helioseismic instruments aboard SoHO), scientists have been able to find signatures of their presence. However, the individual detection of such modes remains evasive. In this article, we study the signal at 220.7 μHz which is a peak that is present in most of the helioseismic data of the last 10 years. This signal has already been identified as being one component of a g-mode candidate detected in the GOLF Doppler velocity signal. The nature of this peak is studied in particular using the VIRGO/SPM instrument aboard SoHO. First we analyse all the available instrumental data of VIRGO and SoHO (housekeeping) to reject any possible instrumental origin. No relation was found, implying that the signal has a solar origin. Using Monte Carlo simulations, we find, with more than 99% confidence level, that the signal found in VIRGO/SPM is very unlikely to be due to pure noise.

Subject headings: Sun: helioseismology - Sun: Oscillations

1. Introduction

Helioseismology has probed the interior of the Sun over the last three decades. Combining the information provided by several hundred pressure-driven modes (p modes), it has been possible to put constraints on our knowledge of the structure and the dynamics of the solar interior (Christensen-Dalsgaard 2002; Thompson et al. 2003). Unfortunately, only a small fraction of these modes reaches the solar core. Moreover, due to the increase in sound-speed velocity with depth, these modes give little information on the deeper layers as they spend less time there than in the convection zone. Let us take as an example the internal rotation rate of the Sun: the rotation profile is very well known in the convective zone (Thompson et al. 1996; Schou et al. 1998;

---

[1] Instituto de Astrofísica de Canarias, E-38205 La Laguna, Tenerife, Spain

[2] Service d'Astrophysique CEA/DSM/DAPNIA, CE Saclay, 91191 Gif-sur-Yvette CEDEX, France

Howe et al. 2000; Antia & Basu 2000), while the uncertainties grow in the radiative zone and towards the core of the Sun (Jiménez et al. 1994; Elsworth et al. 1995; Couvidat et al. 2003; Chaplin et al. 2004; García et al. 2004). In order to put new constraints inside the solar core other kinds of modes are needed: the gravity (g) modes. For example, by measuring just a few of such modes, information on the core rotation rate can undoubtably be obtained (Mathur et al. 2008), whereas the deepest layers that could be probed using only p-modes are around 0.2 $R_\odot$ (García et al. 2008c).

Gravity (g) modes are buoyancy-driven modes that have the advantage of propagating inside the entire radiative region. However, these waves become evanescent in the convective zone and reach the solar surface with tiny amplitudes preventing us to detect them easily (see for example Belkacem et al. (2008) and references therein). Indeed, several claims for g-mode detections have been made in the past (Delache & Scherrer 1983; Pallé & Roca-Cortés 1988; Thomson et al. 1995); however, modern and better data sets cannot confirm them.

In 1995 was launched the Solar and Heliospheric Observatory (SoHO), one of whose scientific objectives was the detection and characterization of gravity modes (Domingo et al. 1995). Recently, using data from the Global Oscillation and Low Frequency (GOLF) instrument (Gabriel et al. 1995), the signature of the asymptotic properties of ℓ=1 dipole g modes has been measured with a high confidence level (García et al. 2007, 2008a). This signal was also found (García et al. 2006) using photometric data from the Variability of solar IRradiance and Gravity Oscillations (VIRGO) experiment (Fröhlich et al. 1995). Even if certain constraints can be imposed on the structure (García et al. 2008b) and dynamics (García et al. 2007) of the solar core thanks to the study of these asymptotic properties, it is extremely important to detect individual g modes. After 10 years of observations, the level of noise at 200 μHz has been established at $\sim$ 4.5 mm/s when individual peaks are looked for and at 1.5 mm/s when this research is done for multiplets (Elsworth et al. 2006). Indeed some peaks and patterns could be identified as potential gravity modes or mixed modes above the noise level (Gabriel et al. 2002; Turck-Chièze et al. 2004; Mathur et al. 2007) but it has been impossible to tag them unambiguously with the correct ℓ, m and n.

In this paper we analyse a peak around 220.7 μHz that has been studied several times as part of a g-mode candidate using different instruments on board SoHO (see for example Gabriel et al. (1999); Finsterle & Fröhlich (2001); Turck-Chièze et al. (2004); Mathur et al. (2007)) but also from the theoretical side (see for example Cox & Guzik (2004) and references therein). To do so, we start in section 2 with a brief description of the helioseismic instruments used in this work and we analyse in detail the data of the VIRGO/SPM instruments (section 3). In section 4, we look for an instrumental origin for this peak without success by analysing all the housekeeping parameters of the VIRGO package as well as the SoHO pointing. Once it is stablished that this peak seems to have a solar origin we check for its presence in all the other instruments of the VIRGO package (section 5) and in the velocity instruments GOLF, MDI and GONG (section 6). We then finish by discussing its possible nature.

2. Instrumentation and data analysis

The data of VIRGO (Variability of IRradiance and Gravity Oscillation), GOLF (Gravity Oscillation at Low Frequencies) and MDI (Michelson Doppler Imager) on board SoHO (Solar and Heliospheric Observatory) satellite have been used in this research together with the GONG (Global Oscillation Network Group) ground-based netwok.

2.1. SoHO/VIRGO

The VIRGO package was designed to study the characteristics of pressure and internal gravity modes by observing irradiance and radiance variations, to measure the solar total and spectral irradiance and to quantify their variability (Fröhlich et al. 1995, 1997). It is composed of three different types of sensors:

- Two types of absolute radiometers (one VIRGO/DIARAD and two VIRGO/PMO6-V) for the measurements of solar total irradiance and its variations with high accuracy and precision. The cadences of VIRGO/DIARAD and VIRGO/PMO6-V are 180s and 60s respectively.
- Two 3-channel sunphotometers (SPM), one permanently exposed to sun lght and another for backup, set at at 402 nm (blue), 500 nm (green), and 862 nm (red), looking at the Sun as a star with a 60 s cadence. The bandwidth of the filters is 5 nm.
- One Luminosity Oscillation Imager (VIRGO/LOI) for the measurements of the radiance in 12 pixels over the solar disc. The filter is at 500 nm with a bandwidth of 5 nm.The cadence is 60s.

In 1998 June, *SoHO* was lost for several months, but, after a search campaign, was finally found and resumed operations around 1998 October. The VIRGO data after *SoHO*'s "vacations" show the same high quality as before the temporary loss of the probe.

2.2. SoHO/GOLF, SoHO/SOI/MDI and GONG

- SoHO/GOLF is a resonance scattering spectrophotometer (Gabriel et al. 1995, 1997) that measures the line-of-sight velocity using the sodium doublet, similar to the IRIS and BiSON ground-based networks. The GOLF window was opened in 1996 January and became fully operative by the end of that month. Over the following months, occasional malfunctions in its rotating polarizing elements were noticed that led to the decision to stop them in a predetermined position; truly non-stop observations began by 1996 mid-April. Since then, GOLF has been continuously and satisfactorily operating in a mode unforeseen before launch, showing fewer limitations than anticipated. The signal, then, consists of two close monochromatic photometric measurements in a very narrow band (25 mÅ) on a single wing of the sodium doublet. This signal has been calibrated into velocity (Ulrich et al. 2000; Garcia et al. 2005) and is indeed similar in nature to other known velocity measurements, such as those of IRIS and BiSON (Pallé et al. 1999). The sampling of the GOLF data used in this paper is 60 s. Before *SoHO*'s vacations (1998 June), GOLF data were obtained in the blue wing of the sodium line; thus, after the *SoHO* vacations the GOLF team decided change to the red wing of the sodium line (see García et al. 2005, for the latest report on the GOLF instrument).

- The Solar Oscillations Investigation (SOI) uses a Michelson Doppler Imager (MDI) type of instrument (Scherrer et al. 1995). MDI consists of a pair of tunable Michelson interferometers, which image the Sun onto a 1024 pixel x 1024 pixel CCD camera in five wavelengths across the Ni i 676.8 nm line. These resolved data can be processed by forming a weighted combination of the pixel signals to yield a proxy for a Sun-as-a-star response (see Henney (1999)).
- The ground-based Global Oscillation Network Group (GONG; Harvey et al. 1996) consists of six sites, with instruments that use the Fourier tachometer approach to observe the Doppler shift, in the Ni i line, with 1024 pixel resolution. Here, a Sun-as-a-star proxy was formed from a simple integration over all pixels with a cadence of 60s.

3. The 220.7 μHz peak seen in VIRGO/SPM

A long time series of 4098 days of VIRGO/SPM data has been used in this work starting on 1996 April 11. As our purpose is to study the time evolution of signals at low frequency, a total of five independent subseries of 800 days have been computed. Data were available to allow a 50 day shift up to June 2007. These 66 overlapped series were used only for plots while non-overlapping data were used as input for the statistical tests we have carried on.

The slow trends in the time series, due to the degradation in the instruments and long-term solar variability, have been removed by applying a running mean filter of one day. To check whether this filter could affect the detected signal, we have also used a backwards difference filter, in which every measured point is substituted by the difference of two consecutive points $\delta f_n = f_{n+1} - f_n$. To recover the correct amplitudes in the power spectrum, this latter should be divided by the transfer function of the filter $Q(\nu)$, defined as follows (García & Ballot 2008):

$$Q(\nu) = [2sin(\pi\nu\Delta t)]^2 \qquad (1)$$

ν being the frequency and Δt the sampling of the data.

Both filters gave the same results and, in the rest of this paper, we work only with the time series filtered by the 1-day running mean.

We therefore computed several power density spectra using a Fast Fourier Transform (FFT) algorithm and built the time-evolution power diagrams used in this work. Each of them has been computed from the time series which have been extended by four equal time intervals of zero signal . This oversampling makes it easier to detect the bins in which the power is concentrated (Gabriel et al. 2002). We also verified that a sine wave fit (SWF), computed in steps of 0.0001 μHz between 220.5 and 221 $muHz$, yields the same results. Therefore, we have used the normal zero-padded FFT as it is much faster than the SWF.

The time-evolution power diagrams are built as follows: The 66 power spectra of the overlapped time series are computed and plotted vertically using a colour scale for the power. The vertical axis is the frequency of the power spectra with the colour equivalent to the power as indicated on the right-hand side of the diagram and the horizontal axis the number of the time series from 0 to 65, i.e. the time span corresponding to the time series. Looking these time-evolution power diagrams we know at which frequency and for how long a signal can have enough power to be observed above the noise level.

In figure 1 the time-evolution of the three VIRGO/SPM channels are shown for the frequency range 220.5–221.0 μHz. The x-axis spans 11 years of the SoHO mission. A clear signal is observed in the blue channel (top) at around 220.7 μHz, which is stable in time with power that goes from 6–7 to 16–17 ppm^2/μHz. Around time series 60 this signal seems to change its frequency slightly by around 0.3 μHz. In the green and red channels the same continuous signal is visible as in the blue one but with the expected decrease in power with wavelength. It is also important to note that in all these VIRGO/SPM channels a second high-amplitude signal is visible at ~ 220.64 μHz, parallel to the previous one, from time series 20 until the last one but with a small gap between time series 44 and 48.

3.1. Confidence levels and Monte-Carlo simulations

In the previous section we saw that there is a persistent signal around the target frequency of 220.7 μHz. Indeed, the VIRGO/SPM blue channel power density spectrum of the full length time series (see Figure 2) shows the presence of a peak at a precise frequency of 220.667 μHz above the 90% confidence level computed in a 10 μHz window following Appourchaux et al. (2000).

Using subseries of 800 days and a frequency window of 10 μHz, the power level above which an observed peak has a 90% probability not due to noise is 8.87σ (e.g. see Appourchaux et al. (2000)). In the case of zero-padded data, the points are no longer independent and are correlated. Therefore, Monte-Carlo simulations should be used to derive a correction for the above-mentioned confidence level. In our case, for a padding factor of 5 we have added a correction of $\ln(2.8) = 1.03$ derived by Gabriel et al. (2002) to the threshold computed using non-zero-padded data. In this conditions the 90% confidence level at around 9.9σ. Using the VIRGO/SPM blue channel, we found that the peak we are studying has a maximum power in a range between 8.74 and 10.4σ considering only five indepen-

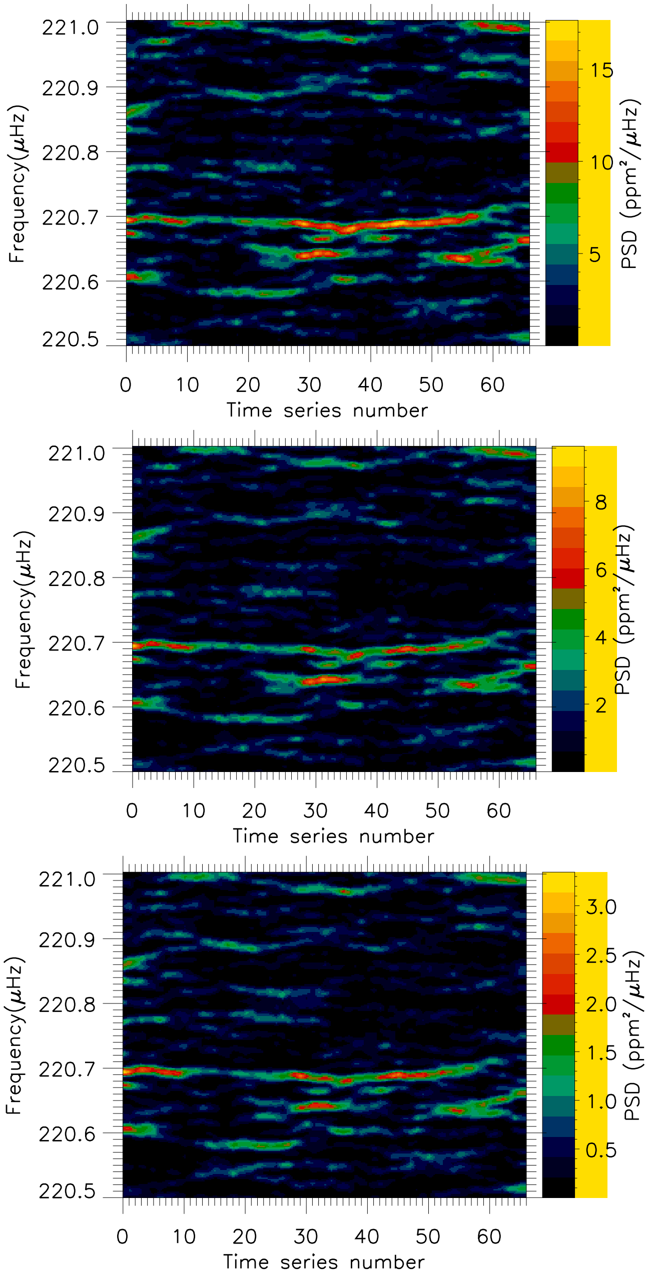

Fig. 1.— VIRGO/SPM time-evolution power diagram of channels blue, green and red (top to bottom respectively) from April 1996 to June 2007. A stable signal at 220.7 μHz is clearly observed.

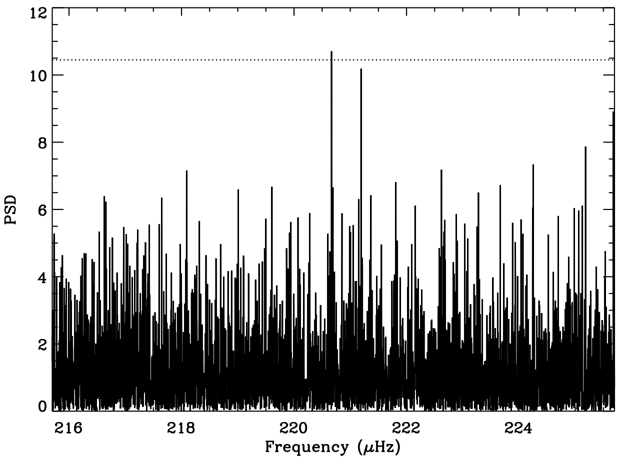

Fig. 2.— VIRGO/SPM blue channel power spectrum density computed with 4098-day time series starting on 1996 April 11. The horizontal dotted line corresponds to the 90% confidence level that a peak above this line would not be due to noise.

dent realizations of 800 days. In Figure 1 the 90% limit is obtained at around 14 ppm^2/μHz (orange colour in Figure 1). This means that, for example, most subseries between the 28th and the 58th have the peak above the 90% confidence level, as well as other subseries such as those at the very beginning of the time-span. It is important to notice that in this case the σ has been averaged over the 66 time series and the value of 14 ppm^2/μHz is an averaged magnitude.

We are interested in knowing the probability of having a signal with the same properties to those that we have found in the VIRGO/SPM blue channel; i.e. a peak that is above the 90% level in the full power density spectrum of more than 4098 days, and that is also present in the five independent subseries of 800 days with similar levels to what we have with this instrument (i.e. not necessary all above a 90% confidence level in these individual small subseries but around that level). This latest condition would be much more restrictive because it means that the peak should maintain a certain coherence during the full time-span. A Monte Carlo simulation of 1 million iterations has been done by simulating Gaussian noise time series of 4000 days that have been cut into five intervals of 800 days. To speed up the procedure we have not computed the full spectrum of the 4000 days but only the average of the power density spectrum of the five independent realizations of 800 days (which have an SNR of $\sim 9.2\ \sigma$ in the VIRGO/SPM blue channel). Thus, the algorithm looks first for a signal in the average spectrum with ∼0.9 times the level found in the VIRGO/SPM blue channel (8.3σ) and, if it is found, it looks for the presence of that signal in the five subseries (again with levels of 0.9 times those of VIRGO). Any signal with these properties found in the 10 μHz window will be flagged as a positive identification. The results show that, in a window of 10 μHz, the 220.7 μHz signal has a likelihood of 99.8% (which is reduced to 91.3% if we only consider the constraint on the averaged spectrum). We have also checked how the likelihood is degraded when a bigger window is considered. Thus, for the 20 and 30 μHz windows we obtain 99.6 and 99.4% respectively.

We can conclude that it is extremely difficult to find a pure noise signal above the 90% confidence level after ∼4000 days and with a coherence with time as found in the VIRGO/SPM instruments.

4. Possible instrumental origin of the signal inside VIRGO and SoHO

Once this interesting signal has been detected in VIRGO/SPM the main question is to investigate its origin; in other words, determine if it is of solar or instrumental origin. In this section, we study all the possible non-solar origins of this signal, from the orbital and pointing corrections of the spacecraft to the housekeeping parameters (hereafter HK) of the VIRGO package.

Periodic manoeuvring of the SoHO probe at this frequency (220.7 μHz, i.e. a period around 1.25 hours) due to orbital adjustments or pointing corrections could modulate the signal of the instruments on board as a tracking system can produce guided frequencies. On the other hand, a temperature variation at this frequency could also modulate the observed signal. These temperature variations could originate in the sensor itself or in other instrument subsystems.

For all these parameters we follow the same analysis we as for the VIRGO data; thus, we build the corresponding time-evolution power diagrams and we compare them with the VIRGO/SPM ones. If the 220.7 μHz signal is produced by the temporal variations of some of these parameters, the time-evolution power diagrams of both VIRGO/SPM and the parameter must be highly correlated.

For this purpose we analyse in the following subsections orbital and pointing corrections of the SoHO spacecraft and the different HK parameters of the VIRGO package that might modulate the signal. It is important to note that some of the

HK data are in the scientific telemetry of VIRGO and have a cadence of 60s, while others are in the HK telemetry and have a cadence of 180s.

4.1. Orbital corrections

The radial distance is reduced to 1AU by the usual quadratic law $S_0 = S \cdot r^2$, r being the spacecraft-to-Sun distance in astronomical units. This correction normalizes the spectral irradiance to the solar constant definition and removes signal modulations due to movements of the Earth, Moon and planets in their orbits.

The observed radiation S of a moving blackbody source is

$$S = S_0 \frac{(1-v)^2}{(1-v^2)} \tag{2}$$

where S_0 is the radiation in motionless conditions and v is the speed in units of the light speed, c. With SoHO velocity being a few 10^{-6} of the speed-of-light one can safely omit terms in v^2 and thus approximate the reciprocal formula

$$S = S_0 \frac{(1-v)^2}{(1-v^2)} \sim \frac{S_0}{(1-2v)} \sim S_0(1+2*v) \tag{3}$$

This Doppler correction removes a tiny (10^{-5}), slow (Halo orbit period is 6 months) modulation of the measured irradiance.

In this way, the orbital correction applied to the three channels of VIRGO/SPM is:

$$SPM_{channel} = SPM_{channel} \cdot radius^2 \cdot (1+2 \cdot vel) \tag{4}$$

where "radius" is the spacecraft-to-Sun distance in astronomical units and "vel" is the radial velocity in units of the speed-of-light.

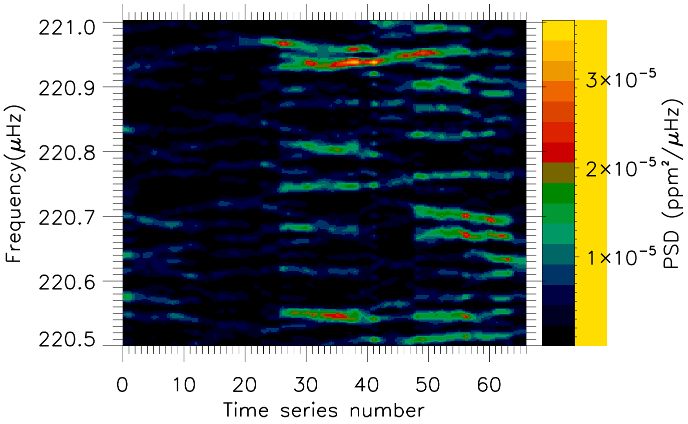

Fig. 3.— Time-evolution power diagram of the orbital corrections applied to the VIRGO data. In addition to the order of magnitude which is 6 orders of magnitude smaller than VIRGO/SPM no correlation is found.

The orbital parameters (radius and vel) are provided by NASA in a 10 minute cadence and are linearly interpolated to get the same 60s as VIRGO/SPM. The time series of the orbital correction applied, i.e. $radius^2(1+2 \cdot vel)$, has been analysed in the same way as VIRGO/SPM and the resulting time-evolution power diagram diagram is shown in Figure 3. The orbital correction signal is around 6 orders of magnitude smaller than the VIRGO/SPM one and no correlation has been found.

4.2. Spacecraft Pointing

The three critical flight dynamics parameters are rotations in three dimensions around the vehicle's coordinate-system origin, the centre of mass. These angles are pitch, roll and yaw. Pitch is the rotation around the lateral or transverse axis. Therefore, movements of the spacecraft to the north or south of the Sun. Yaw is

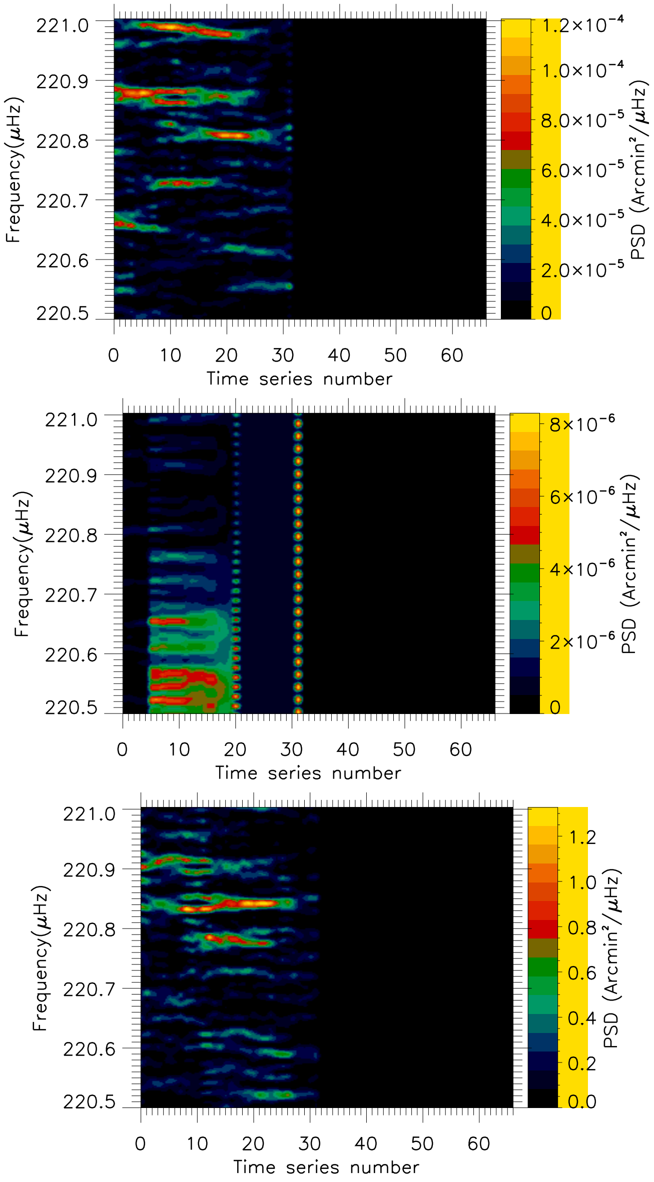

Fig. 4.— Power time-evolution diagrams of the pitch, yaw and roll angles (respectively from top to bottom) of the SoHO spacecraft. Only data up to September 2002 (time series 32) are available. No correlation with the first 32 time series of VIRGO/SPM is found.

the rotation about the vertical axis; thus, movements of the spacecraft to the west or east of the Sun and, finally, roll is a rotation around the longitudinal axis i.e. movements of the spacecraft from the north or south to the west or east of the Sun.

For an instrument that looks at the Sun as a star (integrated light) the most plain pointing correction would be divided by $cos(\sqrt(yaw^2 + pitch^2))$, i.e. the cosine of the angle between instrument optical axis and the line-of-sight direction. Nevertheless, this correction was never applied to VIRGO/SPM because the correction would have been negligible. Also, in December 2001, NASA discontinued the CDHF (Central Data Handling Facility), which was the facility in charge of processing, producing and distributing the SoHO telemetry and the ancillary data products. The production of all these data were continued in others ways but the production of attitude data was stopped in September 2002. Indeed, when SoHO is in normal mode, the attitude follows nominal attitude well enough for most purposes, and because the roll determination had large errors (because of certain procedural problems).

Even knowing that, it would be very unlikely that the pointing maneuvres could modulate any signal in the SoHO instruments; the three angles have been analysed and their time-evolution diagrams computed (see Figure 4).

The available attitude data concerning pitch, yaw and roll angles were obtained from the NASA archive from 1996 April 11 to 2002 September 22 and we built the time series of the three angles. These data have a cadence of 10 minutes and have been used with this sampling rate because it is good enough for our purposes. The length of these time series enables us to get 32 time series of 800 days (each shifted 50 days with respect to the previous one). This is approximately half of the time-evolution power diagrams used in the VIRGO/SPM. This length is sufficient to see if any correlation exists between pointing and SPM signals during the common period (around 6 years).

The pitch angle has a very constant value of around -3.3 arcmin during the time span, with spikes of 5 arcmin and only a few of them with higher values, between 6 and 13 arcmin. These latter are probably due to spacecraft maneuvres. The associated time-evolution diagram is shown in Figure 4 (*top*). Some power density has been found at a level of $10^{-5}(arcmin)^2/\mu$Hz with no visible correlation with the VIRGO/SPM signal.

The yaw angle is zero during practically the whole time-span considered with some spikes around 1.7 arcmin and only a few between 6.8 to 12 arcmin. This yields a pure noise time-evolution diagram (see Figure 4 (*medium*)) with a power density of around $10^{-6}(arcmin)^2/\mu$Hz with also no visible correlation with the VIRGO/SPM signal.

Finally, as we have already said, the roll angle does not affect the data achieved by instruments that observe the Sun as a star (integrated light) but, in any case, it has also been analysed. The roll angle changes following the Earth orbit between 7.16 and -7.16 degrees with some large spikes that have been removed (the roll angle sometimes has large errors) and the time-evolution diagram is shown in Figure 4 (*bottom*). The power density is around $1(arcmin)^2/\mu$Hz and, once again, no correlation with the measurements of VIRGO/SPM has been found.

4.3. VIRGO/SPM temperatures

- VIRGO/SPM sensor temperatures

  The most important VIRGO/SPM temperature is the temperature sensor. Each of the three VIRGO/SPM channels (blue, green and red) are corrected by a quantity proportional to each of the temperature sensors (sensor blue, green and red). This correction is applied in the level 1 software, so the data we are handling are already multiplied by this quantity. This correction is:

  $$SPM_{channel} = (1+C_{channel}(TS_{channel}-293.15)) \tag{5}$$

  where "channel" means blue, green or red; $C_{channel}$ is a constant for each channel and $TS_{channel}$ is the temperature of each of the three sensors.

  In Figure 5 the time-evolution power diagram of the temperature sensor of the blue channel is shown (top of the right column) . The fluctuation of this temperature is two orders of magnitudes smaller that the VIRGO/SPM signals at frequencies around 220μHz and no clear correlation with VIRGO/SPM signals is visible.

- VIRGO/SPM electronic temperature

  The temperature of the SPM electronics has been also analysed to see if there exists some modulation that

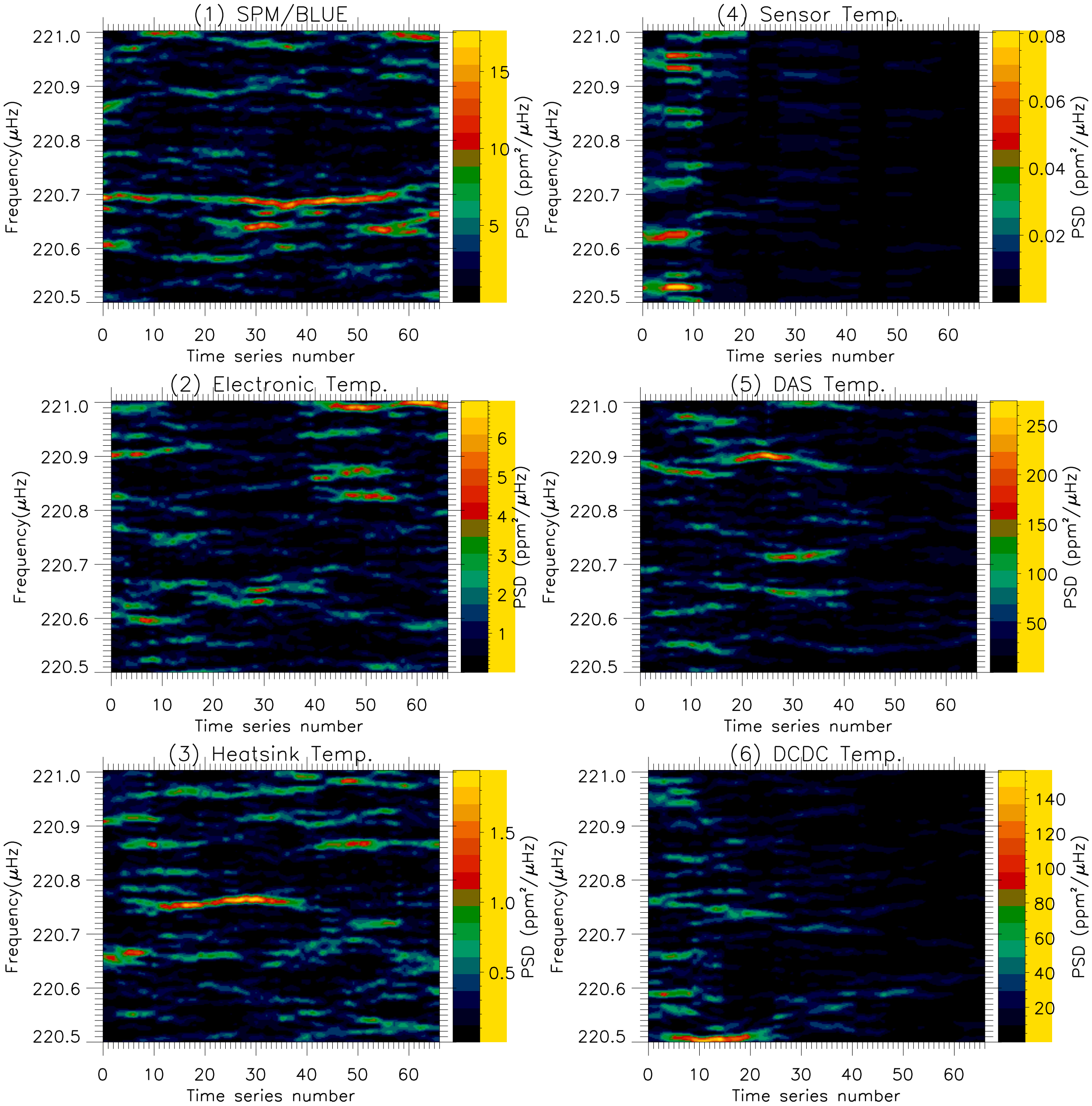

Fig. 5.— Time-evolution power diagram of the HK temperatures of the VIRGO/SPM package. To simplify the comparison we have repeated, on the same scale, the time-evolution diagram of the VIRGO/SPM Blue channel.

could produce a periodic variation in the output voltage of the low-noise electrometer amplifiers (or in the input current). If this exists, a modulation would go to the Voltage Frequency Converters (VFC) of the Data Acquisition System (DAS) and could produce a modulation in the output signal.

The time-evolution power diagram for the VIRGO/SPM electronic temperature is shown in Figure 5 (middle of the left column). The power density is of the same order as in the VIRGO/SPM channels but no correlation with the signal at 220.7 μHz has been found.

- Data Acquisition System (DAS) temperature

  The Data Acquisition System (DAS) of VIRGO comprises the Onboard Data Handling System (interface for telemetry, telecommands and timing signals), multiplexers, Voltage Frequency Converters (VFC) and counters. If the DAS temperature, the VFC or the counters have a periodic behaviour, the output number of counts could contain that periodicity. The DAS temperature time-evolution diagram is shown in Figure 5 (middle of right column). The power density is an order of magnitude higher than the SPM signal but again there is no correlation with the signal at 220.7 μHz .

- VIRGO/SPM Heatsink and DC/DC temperatures

  The temperature variations of the VIRGO Heatsink and the VIRGO Power Supply (DC/DC) have been also analysed for security. The Heatsink time-evolution diagram (Figure 5)(bottom of the left column) is ten times smaller than the VIRGO/SPM and that corresponding to the DC/DC is ten times larger (Figure 5 ,bottom of the right column). In both cases no correlation is found with the 220.7 μHz signal.

  Finally, if a signal is the result of a certain temperature modulation, the temperature variation would be higher just where the power of the signal is higher. In Figure 6 the SPM/Blue and VIRGO HK time-evolution power diagrams are plotted together but only between time series 35 to 55, in which the power of the 220.7 μHz signal is stronger in the VIRGO/SPM data. This zoom helps us to see the darker parts of some HK time-evolution diagrams produced by the colour scales. None of the temperatures analysed in this section can explain the observed signal at 220.7 μHz.

5. The 220.7 μHz signal in the others VIRGO instruments

As was mentioned in section 2.1 the VIRGO package comprises the SPM Sunphotometers and also two types of absolute radiometers (VIRGO/DIARAD and VIRGO/PMO6-V) and one Luminosity Oscillation Imager (VIRGO/LOI). In this section we study the 220.7 μHz signal in these instruments.

- Luminosity Oscillation Imager (VIRGO/LOI)

  VIRGO/LOI measures the radiance in 12 pixels over the solar disc. We convert these 12 pixels into one by simply adding all of them. From the raw time series the same analysis as in VIRGO/SPM has been carried out. Figure 7 (*Top*) shows its time-evolution diagram. It looks similar to the VIRGO/SPM and with the same visible signal at 220.7 μHz. In the VIRGO/LOI observations, the signal is weaker than in VIRGO/SPM but

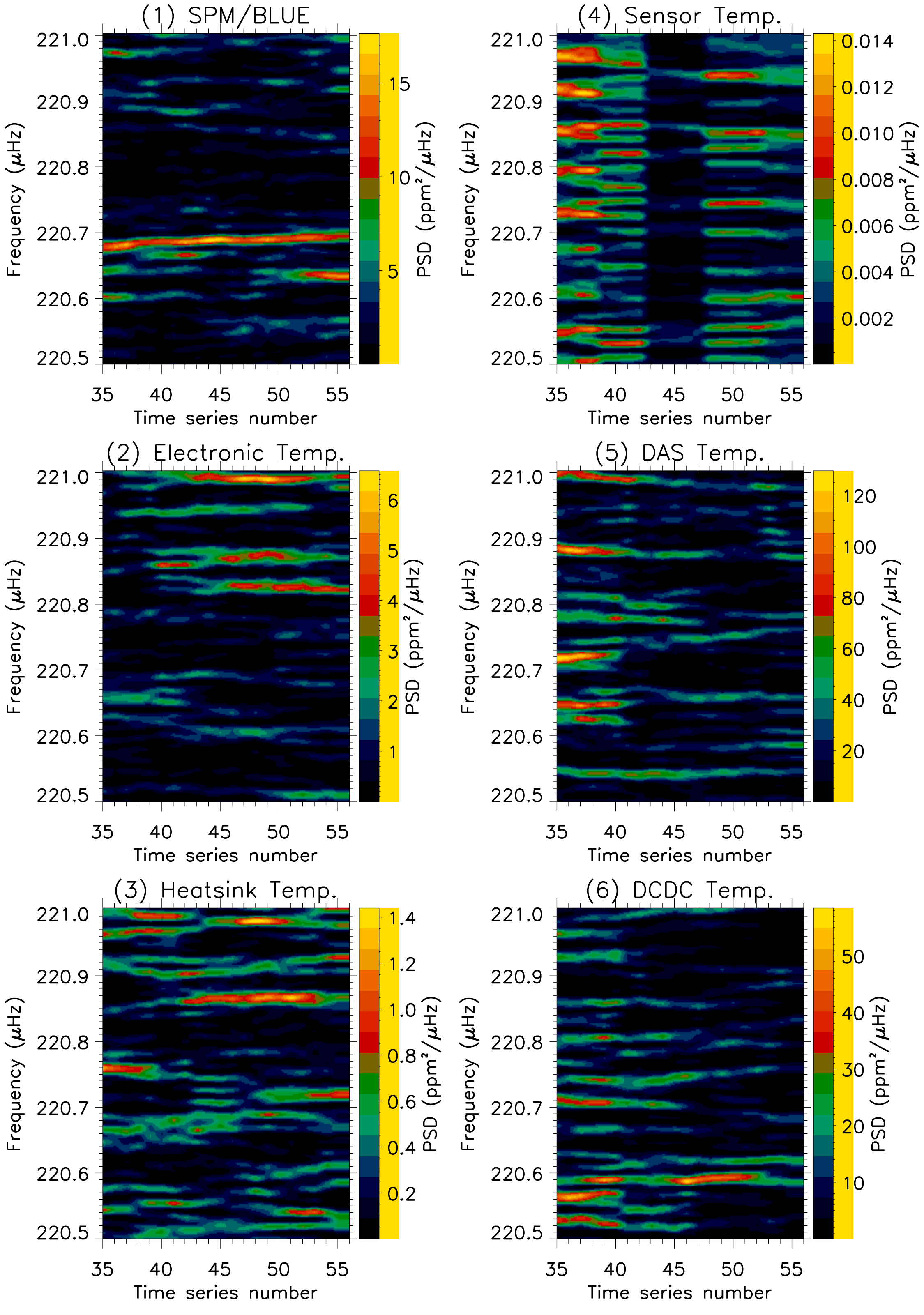

Fig. 6.— Zoom of the time-evolution power diagrams of the VIRGO/SPM Blue and the VIRGO housekeeping analysed in this research for the time series 35 to 55 where the 220.7 μHz has higher amplitudes. This zoom helps to clarify the darker parts of some time-evolution diagrams produced by the colour scales. None of these temperatures can explain the observed signal at 220.7 μHz .

with the same characteristics, for example, at time series 60 the signal slightly changes its frequency. However, with this instrument, the peak seems to be like a doublet instead of only one signal concentrated in a couple of bins.

- Absolute radiometers (VIRGO/DIARAD and VIRGO/PMO6-V)

  Absolute radiometers use a quite different technique from that of VIRGO/SPM and VIRGO/LOI, which are silicon detectors measuring the spectral irradiance and the radiance respectively. Absolute radiometers are based on the measurements of the heat flux by using an electrically calibrated heat flux transducer to measure the total solar irradiance (solar constant). Once again, from the raw time series we have performed the same analysis. Figure 7 (*medium and bottom*) shows the results for VIRGO/DIARAD and VIRGO/PMO6-V. Time-evolution power diagrams are similar to the previous ones, although the 220.7 μHz is weaker in both radiometers but the 220.7 μHz signal is still present.

6. Analysis using Doppler velocity instrumentation

Up to now we have not found any instrumental origin for the 220.7 μHz signal observed in all the VIRGO package. We can now study this region in other helioseismic instruments. We will start by analysing the signal of the other two instruments on board SoHO and we finish by using the

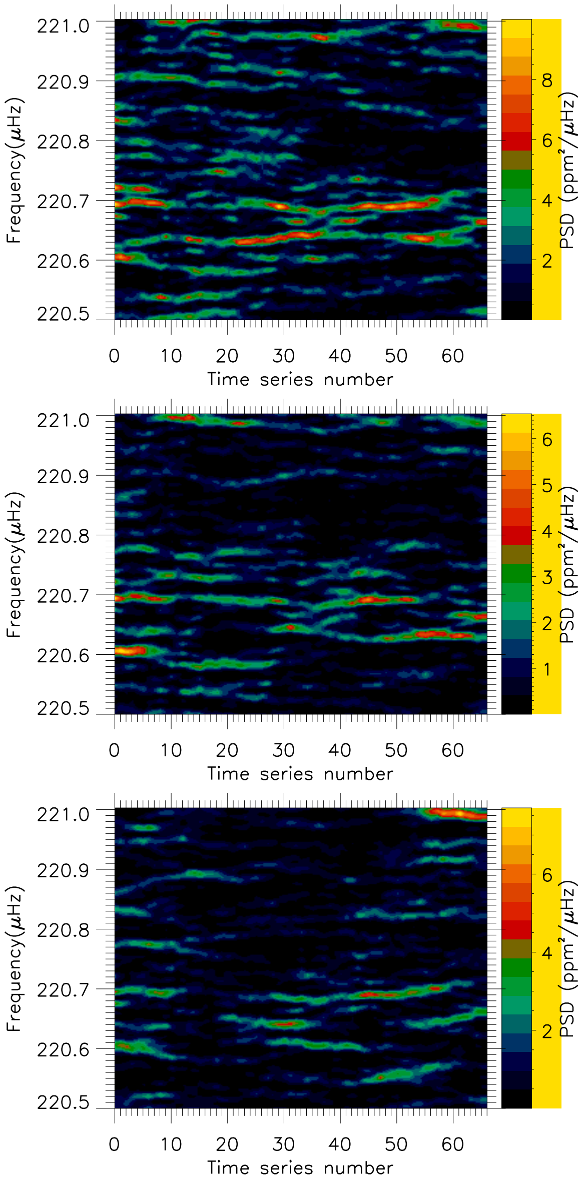

Fig. 7.— Time-evolution power diagram of the Luminosity Oscillation Imager (VIRGO/LOI), the VIRGO/DIARAD absolute radiometer and the VIRGO/PMO6-V absolute radiometer, respectively from top to bottom. All these instruments are part of the VIRGO package.

GONG ground-based network.

- GOLF is the other Sun-as-a-star instrument on board SoHO. We have analysed the velocity time series following the same procedure employed in the VIRGO analysis and we have computed the time-evolution power diagram shown in Figure 8 *(top)*. As mentioned in the introduction, the 220.7 μHz signal was first observed by GOLF during the first years of the mission and it was flagged as a “g-mode” candidate by Turck-Chièze et al. (2004) and, after 4182 days, it is still visible as part of a quadruplet above a 90% confidence level (García et al. 2008a). Figure 8 *(Top)* shows that the evolution with time of the signal, although weaker than in VIRGO, is still there. The signal in GOLF has an interval between time series 12 and 19, where it disappears, and it corresponds to the place where the signal in VIRGO/SPM is the weakest (see figure 1). Therefore, we can conclude that the 220.7 μHz is also observed in velocity measurements using GOLF data but with a smaller signal-to-noise ratio (SNR).

- Disc-averaged MDI velocity signals from the calibrated level-1.4 MDI LOI-proxy Doppler images were obtained using integrated spatially weighted masks following Henney (1999). These time series from 1996 May 25 till 2007 October 28 have been analysed and the time-evolution diagram plotted in Figure 8 *(medium)*. There are no fingerprints

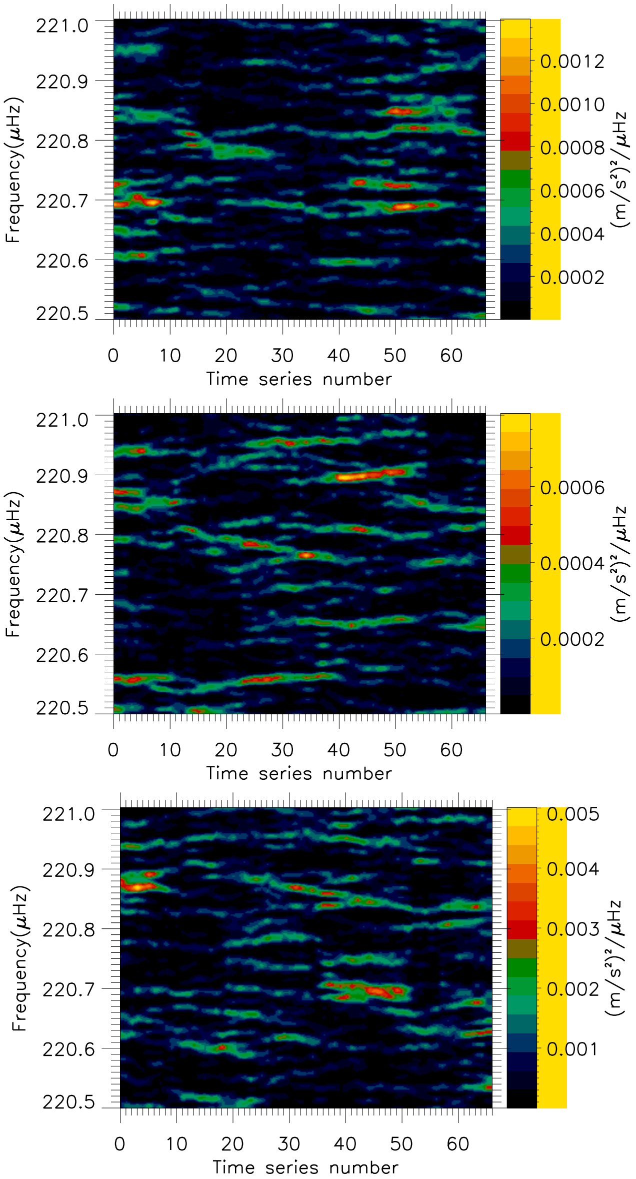

Fig. 8.— Time-evolution power diagram of the GOLF, MDI and GONG instruments respectively from top to bottom.

of the presence of the 220.7 μHz signal in this data set. This could be due to a lower SNR in the MDI LOI-proxy as compared to GOLF. Indeed, Henney et al. (1999) showed that for the lowest measurable p-modes, the GOLF instrument has a higher SNR than this particular MDI mask. To go further, we need to apply our methodology to specifically designed g-mode masks such as those derived by Watcher et al. (2003).

- The radial velocity of GONG used in this work started on 1995 May 7 and finished on 2006 March 9. These series are shifted by a year compared to the SoHO data but they were the longest we could use. The disc-integrated data provided by the GONG Team are very noisy at low frequency and were not suited for our studies. Therefore, we have decided to use the ℓ=2 spherical-harmonic series. These are optimized for acoustic modes of this degree and they have the advantage of having a much stabler behaviour at low frequency. We preferred these series to the ℓ=1 mode because the closest theoretical frequency to the target frequency of 220.7 μHz corresponds to an ℓ=2 g mode. In Figure 8 *(bottom)* the time-evolution diagram of GONG is shown. Although the SNR at this frequencies in the GONG data is very low, it seems to be a trace of the 220.7 μHz signal in the GONG data, especially between series 36 and 52, which corresponds to a maximum in the GOLF between series 43 and 60 (7 subseries shift, i.e. $\sim$ 350 days). However, looking only at this time-evolution diagram, it is impossible to disentangle the feature at 220.7 μHz from others visible in the analysed region. Nevertheless, It would be extremely important to be able to confirm the visibility of such a peak using ground-based data because that would directly mean that the nature of this 220.7 μHz signal has a solar origin.

To compare the averaged behavior of the 220.7 μHz signal in the GOLF, GONG and VIRGO/SPM data sets we computed the collapsograms of the time-evolution power diagram, i.e. to average the 66 power spectra used to produce the time-evolution power diagrams. The resultant graphs are plotted in Figure 9. A similar structure appears around the target frequency of 220.7 μHz, this peak being the highest in the three instruments. However, in the case of GONG, it is at noise level.

7. Conclusions

In the present paper we have studied a peak that appears around the frequency of 220.7 μHz in the VIRGO/SPM data. This peak has a more than 90% confidence level of not being due to noise in the full spectrum of 4098 days. A detailed study of its nature revealed that this peak existed since the very begining of the mission in a continuous way for the last 11 years and only at the very end of the time series considered does it seem to change slightly in frequency. By Monte Carlo simulations we have computed the confidence level of such kinds of behaviour and we found that it is really unlikely (more than

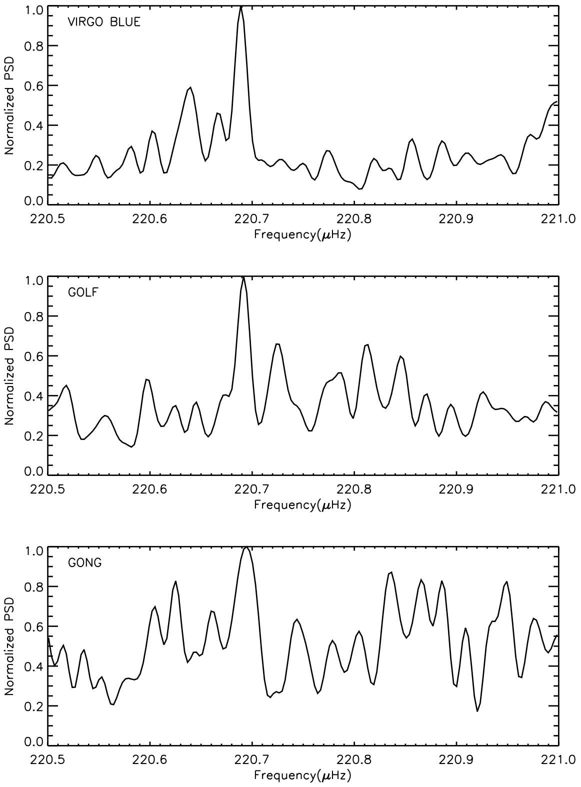

Fig. 9.— Collapsograms of the time-evolution power diagrams of VIRGO/blue, GOLF and GONG. The 220.7 μHz structure is present in the three different instruments although in GONG it is at noise level.

99%) that it is due to a noise with the same statistical characteristics as the convective noise. Therefore, we checked all the available housekeeping data from the VIRGO package as well as a detailed analysis of the SoHO spacecraft attitude control, looking for an instrumental origin. None of these studies was able to explain the presence of a peak in the region studied. Indeed, this study seems to rule out this possibility. The origin should therefore be solar. We then studied Doppler velocity data from another instrument on board SoHO, GOLF, and we found that the peak is also present (with lower SNR). Even though analysis of data from the GONG ground-based network revealed a very noisy spectrum, the highest peak in a 10 μHz region around the 220.7 μHz signal is precisely that peak. However, it is not significant enough for us to claim that we have a positive detection using this instrument.

The present study has proved the solar origin of the peak at 220.7 μHz. Two solar phenomena could be responsible of such a peak. The first could be convection, in particular granulation motions. However, it is very unlikely that a turbulent displacement of plasma on the solar surface with a typical time scale of 10 minutes give a stable frequency during more than 10 years in the power spectrum of the disc-integrated data. On the other hand, gravity modes propagate inside the radiative region of the Sun and are expected to have long lifetimes (at least longer than the period of measurements). Thus, the properties of the peak that we found are similar to those expected for a g mode. Using the principle of Ockham's razor (or the *Lex Parsimoniae* principle) in which the explanation of any phenomenon should make as few assumptions as possible, we can conclude that if this peak is not noise it should be a component of a g mode. Analysing in detail the structure of this possible g-mode component, Figure 2 reveals a peak structure containing several bins. Indeed, Figure 1 might also show the presence of a parallel component at around 220.64 μHz with high amplitudes in several of the series considered. Thus, a possible explanation of such behaviour might be the presence of an inner magnetic field that could slightly split the component of the g-mode multiplet in some peaks. Another possibility might be that the g-mode power could be spread into several bins as a consequence of a smaller than expected lifetime or due to a change in the size of the resonant cavity (for example due to a displacement of the position of the tachocline during the activity cycle). This latter effect is particularly interesting because it seems that the 220.7 signal follows a small change in frequency over the entire time-span with the lowest frequency (220.68 μHz) reached around time series 35—corresponding to the maximum of the activity cycle— and then increasing the frequency again towards the two periods with minimum activity (at the beginning and the end of the series). In any case, assuming a faster rotation in the core than in the rest of the radiative envelope (as suggested by García et al. 2007), the 220.7 μHz peak could be or a component of the ℓ=2, n=-3 g mode, or a component of the ℓ=3, n=-5 or a bitting between this latter and the ℓ=5, n=-8. Whatever the true answer is, there is still an important question to be answered: why is this particular peak so excited when there are no other visible g-mode components? More work will be necessary before solving the solar g-mode puzzle.

The authors want to thank the members of the PHOEBUS group present at the first ISSI (International Space Science Institute) meetings for their useful comments and discussions. This work has been partially supported by the Spanish grant PNAyA2007-62651 and the CNES/GOLF grant at the SAp/CEA-Saclay. The authors also thank all their colleagues (scientists, engineers and technicians) involved with the GOLF, VIRGO and MDI instruments aboard SoHO which is a space mission of international cooperation between ESA and NASA. This work utilizes data obtained by the Global Oscillation Network Group (GONG) program, managed by the National Solar Observatory, which is operated by AURA, Inc. under a cooperative agreement with the National Science Foundation. The data were acquired by instruments operated by the Big Bear Solar Observatory, High Altitude Observatory, Learmonth Solar Observatory, Udaipur Solar Observatory, Instituto de Astrofísica de Canarias, and Cerro Tololo Interamerican Observatory. One of the authors (AJ) would like to thank M.Ortiz for invaluable help with the last part of this article.

REFERENCES

Antia, H. M. & Basu, S. 2000, ApJ, 541, 442

Appourchaux, T. and Fröhlich, C. and Andersen, B. et al. 2000, ApJ, 538, 401

Belkacem, K., Samadi, R., Goupil, M.J., et al. 2009, A&A, 494, 191

Chaplin, W. J., Sekii, T., Elsworth, Y., & Gough, D. O. 2004, MNRAS, 355, 535

Christensen-Dalsgaard, J. 2002, Reviews of Modern Physics, 74, 1073

Couvidat, S., García, R. A., Turck-Chièze, S., et al. 2003, ApJ, 597, L77

Cox, A. N. & Guzik, J. A. 2004, ApJ, 613, L169

Delache, P. & Scherrer, P. H. 1983, Nature, 306, 651

Domingo, V., Fleck, B., & Poland, A. I. 1995, Sol. Phys., 162, 1

Elsworth, Y., Howe, R., Isaak, G. R., et al. 1995, Nature, 376, 669

Elsworth, Y. P., Baudin, F., Chaplin, W., et al. 2006, in ESA SP-624: Proceedings of SoHO 18/GONG 2006/HELAS I, Beyond the spherical Sun, Vol. 18

Finsterle, W. & Fröhlich, C. 2001, Sol. Phys., 200, 393

Fröhlich, C., Romero, J., Roth, H., et al. 1995, Sol. Phys., 162, 101

Fröhlich, C., Crommelynck, D. A., Wehrli, C., et al. 1997, Sol. Phys., 170, 1

Gabriel, A. H., Grec, G., Charra, J., et al. 1995, Sol. Phys., 162, 61

Gabriel, A. H., et al. 1997, Sol. Phys., 175, 207

Gabriel, A. H., Turck-Chièze, S., García, R. A., et al. 1999, Adv. Space Research, 24, 147

Gabriel, A. H., Baudin, F., Boumier, P., et al. 2002, A&A, 390, 1119

García, R. A., Corbard, T., Chaplin, W. J., et al. 2004, Sol. Phys., 220, 269

García, R. A., Turck-Chièze, S., Boumier, P., et al. 2005, A&A, 442, 385

García, R. A., Turck-Chièze, S., Jiménez-Reyes, S. J., et al. 2006, in ESA Special Publication, Vol. 624, Proceedings of SoHO 18/GONG 2006/HELAS I, Beyond the spherical Sun

García, R. A., Turck-Chièze, S., Jiménez-Reyes, S. J., et al. 2007, Science, 316, 1591

García R.A. & Ballot, J. 2008, A&A, 477, 611

García, R. A., Jiménez, A., Mathur, S., et al. 2008a, Astronomische Nachrichten, 329, 476

García, R. A., Mathur, S., & Ballot, J. 2008b, Sol. Phys., 251, 135

García, R. A., Mathur, S., Ballot, J., et al. 2008c, Sol. Phys., 251, 119

Harvey J.W., Hill F., Hubbard R. et al. 1996, Science, 272, 1284

Henney, C. J. 1999, Ph.D. thesis, UCLA

Henney, C. J., Ulrich, R. K., Bertello, L., et al. 1999, A&A. 348, 627

Howe, R., Christensen-Dalsgaard, J., Hill, F., et al. 2000, Science, 287, 2456

Jiménez, A., Pérez Hernandez, F., Claret, A., et al. 1994, ApJ, 435, 874

Mathur, S., Eff-Darwich, A., García, R. A., & Turck-Chièze, S. 2008, A&A, 484, 517

Mathur, S., Turck-Chièze, S., Couvidat, S., & García, R. A. 2007, ApJ, 668, 594

Pallé, P. L. & Roca-Cortés, T. 1988, in IAU Symposium, Vol. 123, Advances in Helio- and Asteroseismology, ed. J. Christensen-Dalsgaard & S. Frandsen, 79

Pallé, P. L., Régulo, C. Roca Cortés, T. et al. 1999, A&A, 341, 625

Scherrer, P. H., Bogart, R. S., Bush, R. I., et al. 1995, Sol. Phys., 162, 129

Schou, J., Antia, H. M., Basu, S., et al. 1998, ApJ, 505, 390

Thompson, M. J., Christensen-Dalsgaard, J., Miesch, M. S., & Toomre, J. 2003, ARA&A, 41, 599

Thompson, M. J., Toomre, J., Anderson, E., et al. 1996, Science, 272, 1300

Thomson, D. J., Maclennan, C. G., & Lanzerotti, L. J. 1995, Nature, 376, 139

Turck-Chièze, S., García, R. A., Couvidat, S., et al. 2004, A&A, 604, 455

Ulrich, R. K., García, R. A., Robillot, J.-M., et al. 2000, A&A, 364, 799

Wachter, R. and Schou, J. and Kosovichev, A. G. & Scherrer, P. H 2003, ApJ, 588, 1199

This 2-column preprint was prepared with the AAS LaTeX macros v5.2.